Schweizerische Eidgenossenschaft
Confédération suisse
Confederazione Svizzera
Confederaziun svizra

Department of the Environment, Transport, Energy and Communication DETEC

Swiss Federal Office of Energy SFOE
Energy Research

Final report August 2018

ReceiverSIM

Modelling of Absorbing Gas Receivers for Solar Applications

Date: August 2018

Town: Manno

Publisher:
Swiss Federal Office of Energy SFOE
XY Research Programme
CH-3003 Bern
www.bfe.admin.ch

Agent:
Synhelion SA
Obere Plessurstrasse 36, CH-7000 Chur
synhelion.com

SUPSI – DTI – MEMTi
Via Cantonale, Galleria 2, CH-6928 Manno
www.supsi.ch ; www.supsi.ch/memti

Authors:
Maurizio C. Barbato, SUPSI – DTI – MEMTi, maurizio.barbato@supsi.ch
Davide Montorfano, SUPSI – DTI – MEMTi, davide.montorfano@supsi.ch
Simone A. Zavattoni, SUPSI – DTI – MEMTi, simone.zavattoni@supsi.ch
Filippo Contestabile, SUPSI – DTI – MEMTi, filippo.contestabile@supsi.ch
Alessandro Pizzoferrato, SUPSI – DTI – MEMTI, alessandro.pizzoferrato@supsi.ch

Gianluca Ambrosetti, Synhelion SA, gianluca.ambrosetti@synhelion.com
Philipp Good, Synhelion SA, philipp.good@synhelion.com

SFOE head of domain: Stefan Oberholzer, stefan.oberholzer@bfe.admin.ch
SFOE programme manager: Stefan Oberholzer, stefan.oberholzer@bfe.admin.ch

SFOE contract number: SI-501618-01

The author of this report bears the entire responsibility for the content and for the conclusions

Swiss Federal Office of Energy SFOE
Mühlestrasse 4, CH-3063 Ittigen; postal address: CH-3003 Bern
Phone +41 58 462 56 11 · Fax +41 58 463 25 00 · contact@bfe.admin.ch · www.bfe.admin.ch

drawn therefrom.

Contents

Project goals

This project aims at the development of a numerical model to simulate an innovative high temperature solar receiver, proposed by Synhelion SA, operating in the 1'000-1'500 °C temperature range. Such receiver is meant for large scale installations (> $1MW_{th}$), with high flux solar towers or (multiple) large dishes. So far, Synhelion has devoted its efforts to validate the innovative receiver concept with a detailed modeling of the radiative heat transfer by using the most accurate and realistic method available. However, this has been done only for the simplest receiver geometry and a simplified fluid flow.

The goal of this project is to extend the modeling capacities from the in-depth codes developed in-house by Synhelion to more flexible Computational Fluid Dynamics (CFD) models that

- take into account the details of the gas fluid dynamics,
- can be applied easily to a more general family of receiver geometries.

Summary

A CFD-based approach was developed with the aim of replicating the thermo-fluid dynamics behavior of the innovative high temperature solar receiver under investigation. The CFD model developed was validated against benchmark results obtained by Synhelion with the most accurate, and most computational expensive, models today available to model radiative heat transfer in participating media: spectral line-by-line Monte Carlo ray tracing.

The CFD model was then exploited to perform several simulations campaign in which the effect of some important parameters, on the overall receiver performance, was evaluated. The parameters considered were: heat transfer fluid mass flow rate, heat transfer fluid entrance angle, gravity (receiver orientation), operating pressure, and concentrated solar flux distribution.

The present report summarizes all the major results obtained in the framework of the ReceiverSIM project covering two main topics:

- development and validation of the CFD modelling approach, suitable to replicate the thermo-fluid dynamics behaviour of this innovative cavity receiver.
- description of the CFD simulations campaign performed, on the reference receiver geometry, with the aim of clearly understanding the physical phenomena that governs the behaviour of the receiver under investigation.

Furthermore, all the planned project deliverables are integrated into the present document. In detail, deliverables D 2.1 and D 2.2 are reported in chapter 3; while, deliverables D 3.1 and D 3.2 are described in chapter 4 and chapter 5 respectively.

List of abbreviations

CFD	Computational fluid dynamics
DO	Discrete ordinates
HF	Heat flux
HTF	Heat transfer fluid
LBL	Line by line
MC	Monte Carlo
RTE	Radiative transfer equation
WSGG	Weighted sum of gray gasses

Work undertaken and findings obtained

1 The absorbing gas receiver concept

Synhelion SA is developing an innovative high temperature solar receiver, operating with gaseous heat transfer fluid (HTF), which, in principle, could work with thermal radiation only as heat transfer mechanism as opposed to conventional gas receivers where convection is the dominant heat transfer mechanism. The key aspect of this receiver is the HTF which must have specific spectral properties: it has to be almost transparent to the high-radiation intensity wavelengths of the solar spectrum and, at the same time, mostly opaque (i.e. strong absorption bands) in the wavelength range of thermal radiation. These characteristics can be obtained by exploiting heteropolar gases such as steam (H_2O) or CO_2. Therefore, if a proper amount of gas is considered, it would be possible to absorb a relevant fraction of thermal radiation emitted by a hot surface.

The working principle of the absorbing gas receiver, graphically represented in figure 1, is similar to the greenhouse effect: a cavity-type receiver is exploited to collet concentrated solar radiation that enters from the aperture, travels along the entire cavity length and is absorbed by a highly absorptive surface (referred as back plate) located at the back of the cavity. As a result, the surface temperature increases starting to re-emit longer wavelength thermal radiation into the cavity. At the same time, a stream of HTF, with the aforementioned spectral characteristics, flows also from the aperture towards the back of the cavity absorbing the thermal radiation emitted by the innermost surface (back plate). This causes the temperature of the HTF to increase as it flows through the cavity reaching the maximum value as it approaches the back plate. At this point, the high temperature HTF leaves the cavity receiver from the outlet section to be used for subsequent processes. In principle, the absorbing gas receiver can work with radiation as the only mode of heat transfer, which is particularly effective at operating temperatures above 1’000 K and yields a potentially high receiver efficiency up to 2’000 K, as Synhelion shows in their manuscript [1]. In addition, since no forced convection is required, the cost and complexity of a convective heat exchanger are removed.

If the receiver is operated with steam at atmospheric pressure, a large cavity of several meters is required in order to ensure a proper number of gas molecules on the path between the back-plate and aperture to absorb a relevant amount of thermal radiation and thereby minimizing the heat losses from the aperture. This renders the absorbing gas receiver readily applicable to large solar fields on the 100 MW scale. Furthermore, the size of the receiver can be downscaled by increasing the operating pressure without affecting performance. Operating pressure and path length are inversely proportional: increasing the pressure by a factor of 10 enables the possibility of reducing the cavity size by the same factor of 10. Accordingly, a solar receiver operated with steam at 10 bars serves the 1 MW scale. At least for the first prototypes the operating pressure is a useful parameter to reduce receiver size despite the well-known structural and operative challenges of pressurized receivers.

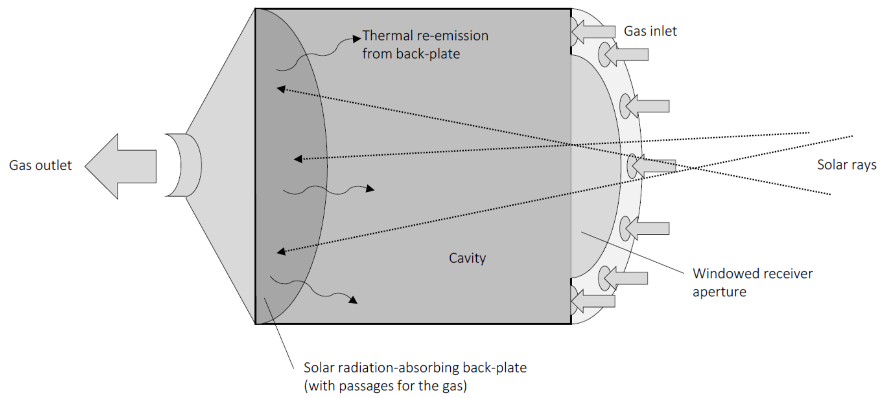

Figure 1: Schematic of the absorption receiver concept [1].

2 Modelling radiative heat transfer in participating media

Thermal radiation heat transfer in flowing “radiatively participating” media (i.e. absorbing, emitting and scattering media), is, by nature, a complicated topic that is normally addressed by means of modelling methods which, depending on the desired accuracy, can be computationally very expensive or applicable to very simple and idealized cases only. The modelling complexity rises with the need of solving the radiative transfer equation (RTE), detailed in [2], which describes how a radiation intensity field varies, within the domain under investigation, as a function of location, direction and spectral variable (wavenumber). Currently, four different methods are commonly exploited for the analysis of radiative heat transfer [3]: (i) the spherical harmonics method, (ii) the discrete ordinates method, (iii) the zonal method and (iv) the Monte Carlo method. In the spherical harmonics method, the RTE directional dependence is not discretized but it is described by a truncated series of spherical harmonics. This method allows to obtain an approximate solution of arbitrarily high order (i.e. accuracy) of the RTE by transforming it into a set of simultaneous, and relatively simple, partial differential equations. Accuracy can be the major limitation of this method since low-order approximation is only accurate in media with almost isotropic radiative intensity. Accuracy increases slowly for higher order approximation while mathematical complexity increases extremely rapidly. The most known approximation belonging to this method is the so-called P1-approximation. The discrete ordinates method can also be used to transform the RTE into a set of simultaneous partial differential equations carried out to any arbitrary order and accuracy. This method is based on a discrete representation of the directional variation of the radiative intensity with the RTE solved for discrete parts (directions) of the total solid angle. In the zonal method, the enclosure is subdivided into a set of isothermal sub-volumes and surface area zones. An energy balance is then applied for the radiative transfer between these zones to derive a set of simultaneous equations for determining the unknown temperatures and heat fluxes. Monte Carlo method is the most accurate, and the most computational expensive, method to evaluate radiative heat transfer. It is a statistical method in which a bundle of photons are physically traced from their point of emission to their point of absorption. As of today [3], the most popular RTE solvers are the spherical harmonics method, with P1-approximation, and the discrete ordinates method; however, Monte Carlo methods have received an increased attention during the past years thanks to the high accuracy, the capability of dealing with effects of irregular radiative properties and the fact that they can be easily adapted for parallel computing.

In the case of participating media, the radiative heat transfer analysis is even more complicated by the fact that spectral variations of the participating media radiation properties have to be taken into account since the gray participating medium assumption (i.e. the radiative properties do not vary across the electromagnetic spectrum) may lead to substantial errors in the analysis. According to Modest [3], exact and approximate methods to evaluate spectral models for radiative heat transfer calculations can be divided into 4 groups: (i) line-by-line calculations, (ii) narrow band calculations, (iii) wide band calculations and (iv) global (gray gas) models. Among the latter, line-by-line is by far the most accurate and complex method relying on very detailed knowledge of every single spectral line (data not always available). The computational effort is remarkable due to the fact that the spectral radiative transfer problem must be solved for up to one million of wavenumbers. For this reasons, line-by-line method has only a very limited applicability in problems of practical interest. The other methods aforementioned, are less complex less computational expensive and less accurate than line-by-line but still reliable enough for a good radiative heat transfer analysis. On the basis of the good compromise between accuracy and computing time, the weighted-sum-of-gray-gases (WSGG) model is the one commonly exploited for deriving the radiative properties (total emissivity and absorptivity) of the participating medium.

The basic assumption of this approach is that the participating medium total emissivity can be computed as the sum of a certain number of fictitious gray gases emissivities properly weighted with a temperature dependent weighting factor. Therefore, the total emissivity over a path length “S” can be defined as [4]:

$$\varepsilon = \sum_{i=0}^{I} \alpha_{\varepsilon,i}(T)\left[1 - e^{-k_i p S}\right] \qquad (1)$$

where “$\alpha_{\varepsilon,i}$” is the temperature dependent emissivity weighting factor of the *i*-th fictitious gray gas, the bracketed quantity represents the *i*-th fictitious gray gas emissivity with absorption coefficient “k_i” and partial pressure-path length product “pS”.

3 Numerical model development and validation

The first part of the project was devoted to the critical analysis of two commercial software products, ANSYS Fluent and ANSYS CFX, with the aim of evaluating their capabilities in modelling radiation in participating media. According to the results of the analysis [2], ANSYS Fluent was selected as reference tool for the development of the proper CFD modelling approach described in the next paragraphs.

3.1 Benchmark Monte Carlo line-by-line (MC-LBL) results

Since at the moment no experimental data is available for the CFD model validation, the outcomes of the MC-LBL model, obtained by Synhelion, were exploited as benchmark results for evaluating the accuracy, reliability, and eventual limitations, of the CFD model especially concerning the simplified spectral radiative properties treatment of the participating HTF.

As shown in figure 2, the computational domain considered for the MC-LBL simulation is a simplified cylindrical cavity operating at ambient pressure (1 bar). The diameters of the cavity and aperture are 15.96 m and 11.28 m, respectively. The surface area of the back plate is 200 m^2 while the aperture area is 100 m^2. The cavity length is equal to its internal diameter, and therefore 15.96 m, leading to an overall internal gas volume of about 3’200 m^3. The gaseous HTF is modelled as an inviscid flow flowing through the cavity in the axial direction only from the aperture and front ring sections to the back plate. The cavity is modelled as ideally insulated and therefore, the only source of heat loss is assumed to be through the aperture by means of thermal radiation only. The internal surfaces of the cavity are considered to have emissivity equal to 1 (black surfaces) and a fully diffusive emission of thermal radiation. A total of 10 simulations were performed considering an inlet temperature of the HTF of 1’000 K and a variable HTF mass flow rate calculated in order to cover a temperature range (T_{out} - T_{in}) of 1’000 K with a resolution of the HTF outflow temperature of 100 K. The resulting receiver thermal efficiency, defined as the ratio of the power removed by the HTF divided by the total input power (concentrated solar radiation) is reported in figure 3.

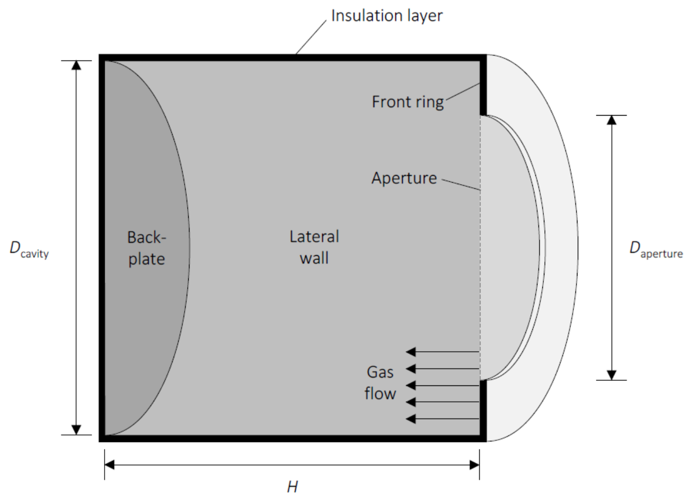

Figure 2: Schematic of the cylindrical cavity receiver assumed for the analysis [1].

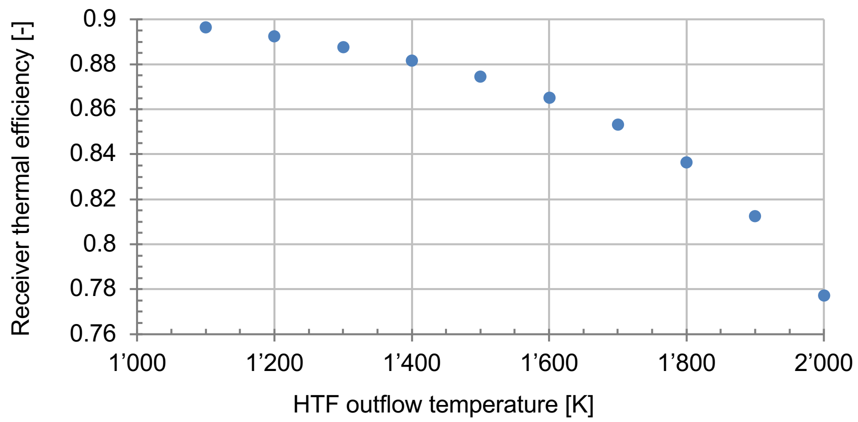

Figure 3: Receiver thermal efficiency as a function of the receiver HTF outflow temperature for the MC-LBL simulation results [1].

3.2 Weighted sum of gray gases (WSGG) model

The development of a reliable and accurate CFD modelling approach to replicate the thermo-fluid dynamics behaviour of the innovative absorbing gas receiver is among the major objectives of the present project since it would allow to evaluate the performance of any generic receiver geometry subjected to any arbitrary boundary conditions. Therefore, fluid flow and heat transfer will be accurately modelled. Concerning the latter, the Discrete Ordinates (DO) radiation model, already available in ANSYS Fluent, was selected for the solution of the RTE. Despite DO is the most demanding model in terms of computational resources, it is at the same time, the only one that allows to model semi-transparent interior or exterior walls (i.e. the receiver aperture), it can be applied for parallel computing and without any restrictions in terms of medium optical thickness [2]. The spectral variation of the participating medium radiative properties was accounted for by the WSGG model. The reference HTF to be considered is pure steam for which the WSGG model coefficients were accurately derived by Synhelion for the foreseen operating conditions of the receiver [1].

3.3 CFD model

3.3.1 Computational domain and discretization

The computational domain considered for the validation process is the same as the one exploited for the MC-LBL simulation (paragraph 3.1). Based upon the geometric characteristics of the simplified receiver design under investigation (Figure 2), and assuming an axisymmetric flow and heat transfer into the cavity, a 2D axisymmetric computational domain was considered for the analysis. As for the MC-LBL model, the computational domain was discretized with a grid of quadrilateral elements with equal length in the axial direction (32 elements) and variable height in the radial direction (16 elements). The variable radial discretization is aimed at providing the same cross-sectional area of each cylindrical cell. For a quantitative CFD analysis, the discretization implemented is rather coarse; nevertheless, for the validation process, it was decided to keep the same discretization for both the models to avoid the risk of having discrepancies in the results due to different computational grids. Figure 4 shows a schematic of the discretized computational domain along with the boundary conditions considered for the simulations.

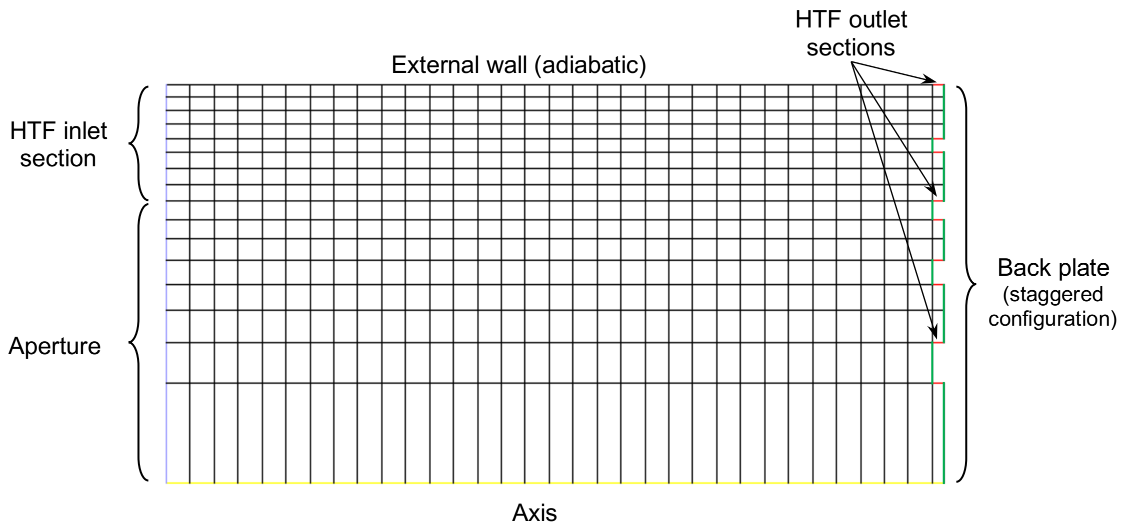

Figure 4: Discretized computational domain considered for the CFD simulations.

3.3.2 Boundary conditions and fluid properties

A mass flow inlet boundary condition was assigned to the HTF inlet section; a homogeneous velocity profile of the incoming HTF was assumed. The HTF inlet temperature was set to 1’000 K. To be as close as possible to the MC-LBL model, a fictitious HTF inlet was also modelled from the cavity aperture. Therefore, in the CFD model exploited for the validation process, the HTF enters the receiver from the entire cavity cross-section (blue edge in figure 4). Concerning the HTF outflow region, multiple outlet sections (red edges in figure 4) were considered with the aim of minimizing the streamline curvature of the HTF flowing through the cavity for maintaining as much as possible the plug flow condition assumed in the MC-LBL model.

The concentrated solar radiation entering the cavity, and impinging on the back plate, is modelled as uniform heat flux (600 kW/m^2) applied on the internal surface of the back plate itself (green edges in figure 4) and therefore, as opposed to MC-LBL model, no ray-tracing is performed during the CFD simulation. The back plate and the lateral wall were assumed to emit diffusely with an emissivity of 1 (black surfaces). The emissivity of the HTF inlet and outlet sections were set to 0 while the aperture was modelled as semi-transparent surface with transmissivity equal to 1.

The receiver was assumed as perfectly insulated (adiabatic condition) with the only heat losses occurring through the aperture by means of radiation towards the ambient (black body) at 300 K and an external surface emissivity of 1.

The HTF was modelled as incompressible ideal gas, i.e. constant density, with a polynomial temperature dependent specific heat (values gathered from CoolProp database) and fictitious values of zero for viscosity and thermal conductivity to accurately replicate the fluid properties considered for the MC-LBL model. Table 1 reports a summary of the main boundary conditions, and material properties, applied to the CFD model for the validation process.

Table 1: Summary of the main boundary, and operating, conditions applied to the numerical model.

HTF			
	density	0.217	[kg/m^3]
	dynamic viscosity	10^{-15}	[Pa·s]
	thermal conductivity	10^{-15}	[W/(m·K)]
	specific heat	f(T) polynomial	[J/(kg·K)]
	mass flow rate (min. - max.)	37.8 – 471.7	[kg/s]
	inlet temperature	1’000	[K]
External conditions			
	ambient temperature	300	[K]
	external emissivity (aperture)	1	[-]
Operating conditions			
	absolute pressure	1	[bar]
	concentrated solar heat flux / power on back-plate	600 / 120	[kW/m^2] / [MW]
	gravity	off	

3.3.3 Numerical details

Apart from the RTE, the CFD model solves the mass, momentum and energy conservation equations in order to have a detailed description of heat transfer and fluid flow within the computational domain.

SIMPLE algorithm [5] was exploited to couple the pressure and velocity fields and to solve the pressure correction equation. The pressure values at the cell faces were interpolated through the PRESTO! (PREssure STaggering Option) scheme [6] and the spatial discretization of the transport equations were performed with a first order accurate upwind scheme. It is well known that first order accurate numerical scheme is very diffusive, and therefore not recommended for a quantitative evaluation of the simulations results, but since it was exploited in the MC-LBL model it was decided to follow the same approach to facilitate the validation process.

Convergence was considered to have been achieved when the mass and momentum residuals were below 10^{-5}, the DO and energy residuals were below 10^{-8} and 10^{-9} respectively.

3.4 CFD model validation

To evaluate the capability of the CFD model developed to replicate the behaviour of the absorbing gas receiver under investigation, a set of 10 CFD simulations were performed varying, for each of them, the reference HTF mass flow rate. The CFD simulations results obtained were compared not only with the benchmarking results of the MC-LBL model but also with those obtained with a second and simpler 2D model, still developed by Synhelion, wherein the WSGG model was implemented. Figure 5 summarizes the comparison of the resulting thermal efficiency of the receiver, defined as the ratio of the power removed by the HTF divided by the total input power (concentrated solar radiation), predicted by the three numerical models. On the basis of the results obtained, it is evident that the simplified approach given by the WSGG model leads to a slight overestimation of the receiver efficiency with respect to the more accurate MC-LBL prediction. Furthermore, the receiver efficiency overestimation increases as the HTF mass flow rate decreases; the difference with respect to the benchmark MC-LBL results is of about 2.6% and 5.4% for the maximum and the minimum HTF mass flow rates respectively. Concerning the two models with the WSGG approximation, as expected, a very good agreement (0.38% maximum variation) was observed for the receiver thermal efficiency prediction.

From a graphical standpoint, figure 6 reports the temperature contours within the receiver as a function of some HTF mass flow rate values considered (for helping the reader in the analysis of the images, it might be worth to recall that the HTF flow direction is from the left to the right of the computational domain). The absorption/emission behaviour of the flowing participating gas can be clearly observed by the axial temperature gradient established into the cavity. Therefore, it is also possible to observe that the participating HTF acts effectively as radiation shield minimizing the amount of thermal radiation, emitted by the back plate or by the innermost region of the lateral wall, that reaches the aperture.

As final consideration of the validation process, despite the slight overestimation of the receiver thermal efficiency, the WSGG model resulted to be an appropriate solution for minimizing the computational resources required by keeping, at the same time, a reasonable accuracy of the results.

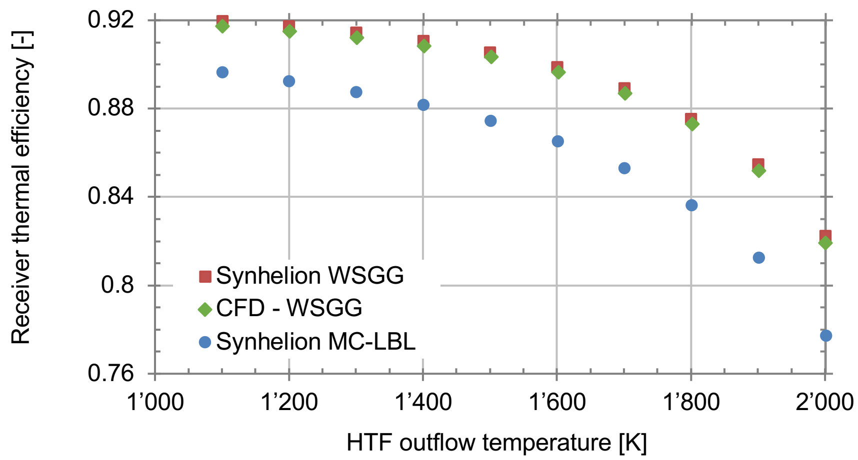

Figure 5: Comparison between CFD simulations results with the reference Synhelion MC-LBL and WSGG simulations results.

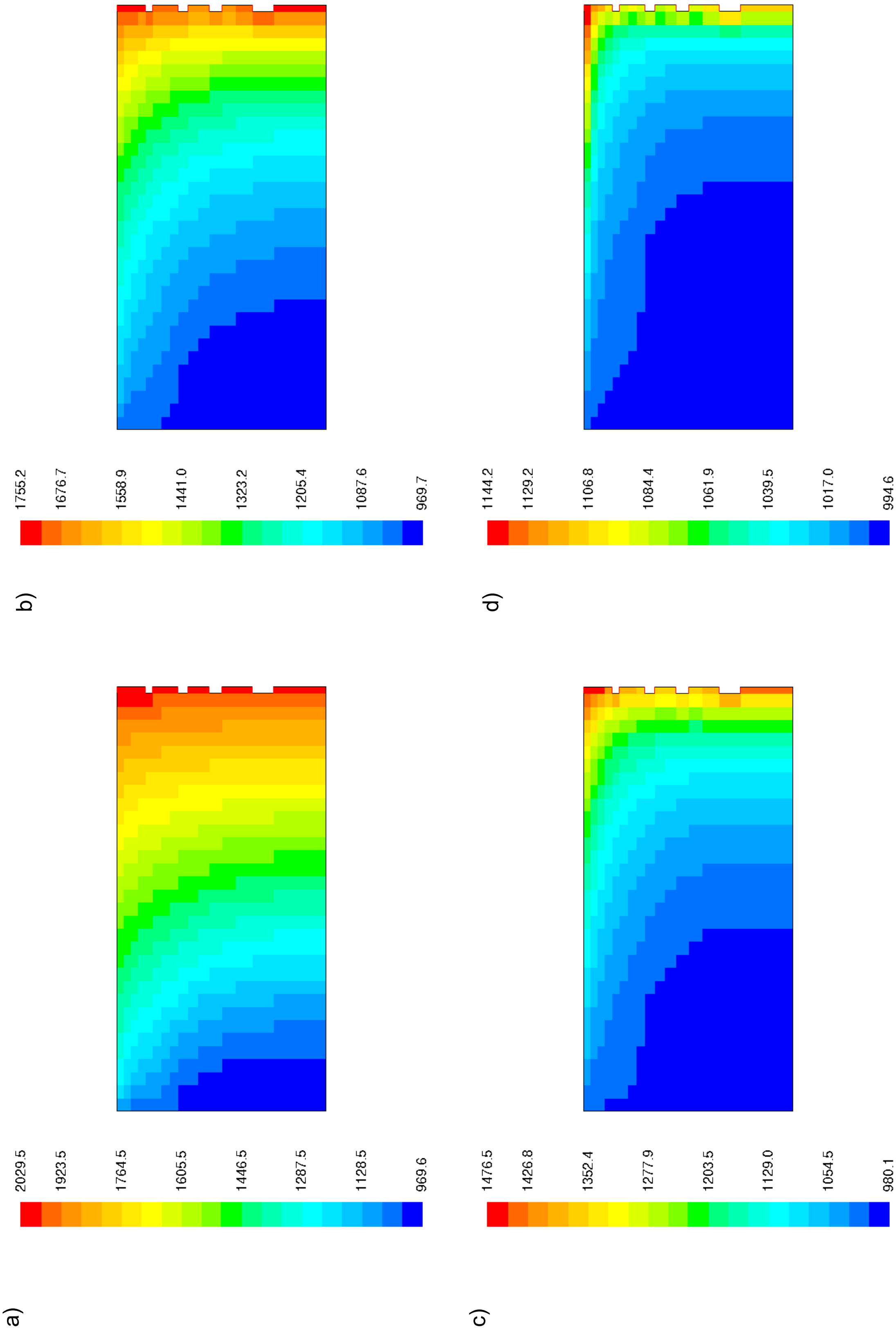

Figure 6: Temperature contours within the receiver for some HTF mass flow rates considered: a) 37.8 kg/s, b) 60.2 kg/s, c) 111.7 kg/s and d) 471.7 kg/s. Temperature values are [K].

3.5 Reference receiver geometry and computational domain

Figure 7 shows the absorbing gas receiver geometry assumed as reference for the CFD simulations campaigns. The internal region of the receiver is composed by two different domains: (i) the cavity domain wherein the absorption of thermal radiation by the participating HTF takes place and (ii) the rear domain in which the high-temperature HTF is guided towards the outlet section. The separation between these two domains is given by the back plate disks.

As previously mentioned for the validation process 3.3.1, in this case also, a 2D axisymmetric computational domain was assumed. It was discretized with a grid of about 90'000 quadrilateral cells. The back plate disks were modelled as flat surfaces, without thickness, but with the possibility of defining different emissivity values on the two sides (towards the cavity domain and vice versa). Since for the initial simulations campaigns the thermal radiation absorption by the participating gas was assumed to take place into the cavity domain only, the emissivity values of the two sides of the back plate, the one facing the cavity domain and the other facing the rear domain, were set to 1 and 0 respectively. For coherence, the emissivity of the rear domain lateral wall was also set to 0. Heat losses were assumed to take place from the aperture only, modelled as semi-transparent surface with external emissivity of 1, by means of thermal radiation towards a blackbody ambient at 300 K.

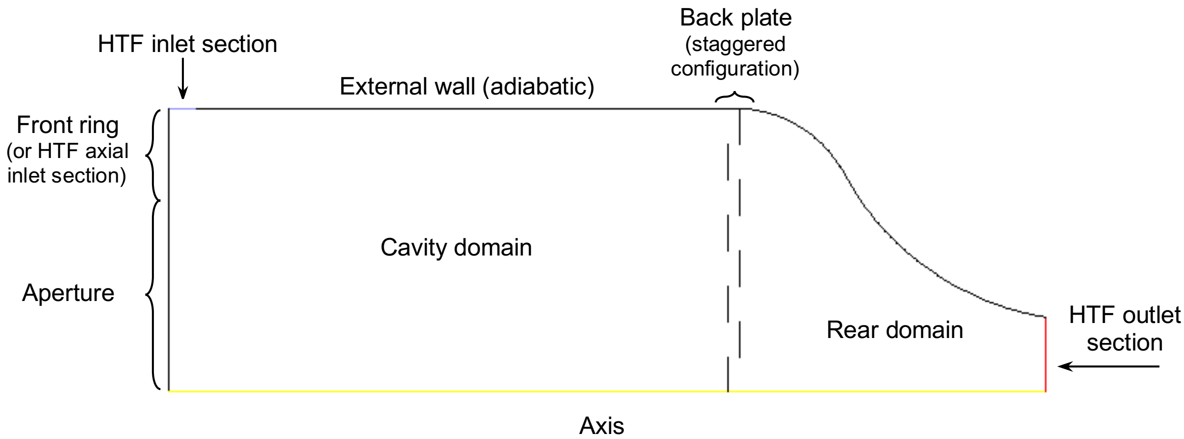

Figure 7: Reference receiver geometry – Computational domain.

4 Results and discussion

In this chapter, the results of various CFD simulations campaigns, performed on basic receiver geometries with the aim of characterizing their performance, will be discussed. In particular, the effect of variable operating pressure on the receiver thermo-fluid dynamics behaviour will be reported and described.

4.1 Atmospheric pressure receiver

In this first CFD analysis, the atmospheric pressure receiver is analysed and, in particular, the effect of the HTF mass flow rate on the absorbing gas receiver performance is evaluated. A total of ten CFD simulations were performed varying any time the HTF mass flow rate keeping the same values already exploited for the validation process. To accurately replicate the temperature dependency of the HTF properties (i.e. dynamics viscosity, specific heat and thermal conductivity) polynomial functions, based on values from CoolProp database with a validity range of 600 K $\geq T_{HTF} \geq$ 3'000 K, were derived and implemented into the solver. Table 2 summarizes the main boundary and operating conditions considered for the CFD simulations campaign.

Figure 8 shows the resulting thermal efficiency of both the reference receiver geometry (red squares), and the idealized receiver of the validation process (green squares), as a function of the HTF outflow temperature. Reducing the HTF mass flow rate leads to a decrease of the receiver thermal efficiency due the higher heat losses. Despite this consideration is valid for both the idealized and the reference receiver geometry, the evolution of the receiver thermal efficiency variation is different. In the case of reference receiver geometry, the efficiency decreases first rapidly as the HTF outflow temperature increases from about 1'100 K to 1'300 K and then stabilizes around the inflection point of 1'500 K. Above 1'500 K the efficiency of the reference receiver geometry follows the same trend as the idealized receiver efficiency, although efficiencies are roughly 6% lower.

The temperature distribution into the receiver, for some of the HTF mass flow rates considered, is depicted in figure 9. Looking at the pictures, it is possible to observe that the temperature stratification into the cavity is sensibly affected by the HTF mass flow rate. When the latter is low, an almost axial temperature stratification is obtained; as the mass flow rate increases, the temperature stratification changes arriving, in the case of the highest HTF mass flow rate, in an almost radial configuration. As expected, the average internal temperature of the cavity is also affected by the HTF mass flow rate in the sense that it reduces as the mass flow rate increases. Furthermore, due to a flow stagnation point, located at the contact region between the outermost back plate ring and the lateral wall, a hot-spot can be observed for all the HTF mass flow rates considered. To mitigate this important temperature gradient in the radial direction of the back plate, a gap between the outermost back plate ring and the lateral wall should be implemented allowing hence the HTF stagnation point to be removed.

As graphically represented by the contours of velocity magnitude depicted in figure 10, the fluid dynamics behaviour of the HTF through the receiver has similar characteristics for all the mass flow rates considered. Based upon the assumed orientation of the HTF inlet velocity vector (27° from the aperture), two important flow recirculation zones can be observed within the cavity domain (Figure 11): the first one in the vicinity of the lateral wall and the other one close to the aperture. A relatively high flow velocity is reached in the outlet region due to a combination of the cross-section reduction of the outlet pipe and the reduced density of the high-temperature HTF.

Table 2: Summary of the main boundary conditions, and material properties, considered for the CFD simulations campaign.

HTF		
density	ideal gas	[kg/m^3]
dynamic viscosity, thermal conductivity and specific heat	f(T) polynomial	[…]
mass flow rate (min. - max.)	37.8 - 471.7	[kg/s]
inlet temperature	1’000	[K]
inlet angle (from aperture)	27	[°]
inlet velocity magnitude (min. - max.)	5.2 - 64.4	[m/s]
Radiative heat transfer		
Back plate:		
concentrated solar heat flux / power on cavity side	600 / 120	[kW/m^2] / [MW]
cavity side emissivity	1	[-]
rear domain side emissivity	0	[-]
Lateral wall:		
concentrated solar heat flux / power on cavity side	0 / 0	[kW/m^2] / [kW]
cavity side emissivity	1	[-]
rear domain side emissivity	0	[-]
Operating conditions		
absolute pressure	1	[bar]
ambient temperature	300	[K]

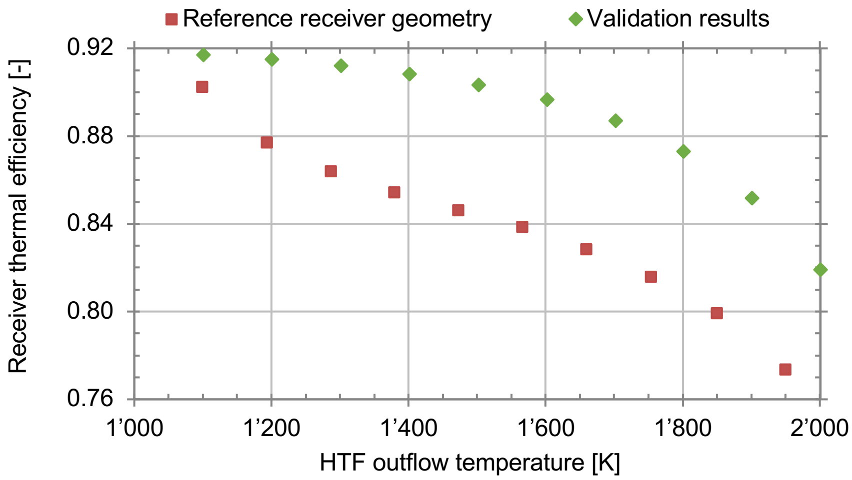

Figure 8: Resulting reference receiver thermal efficiency as a function of the HTF outflow temperature.

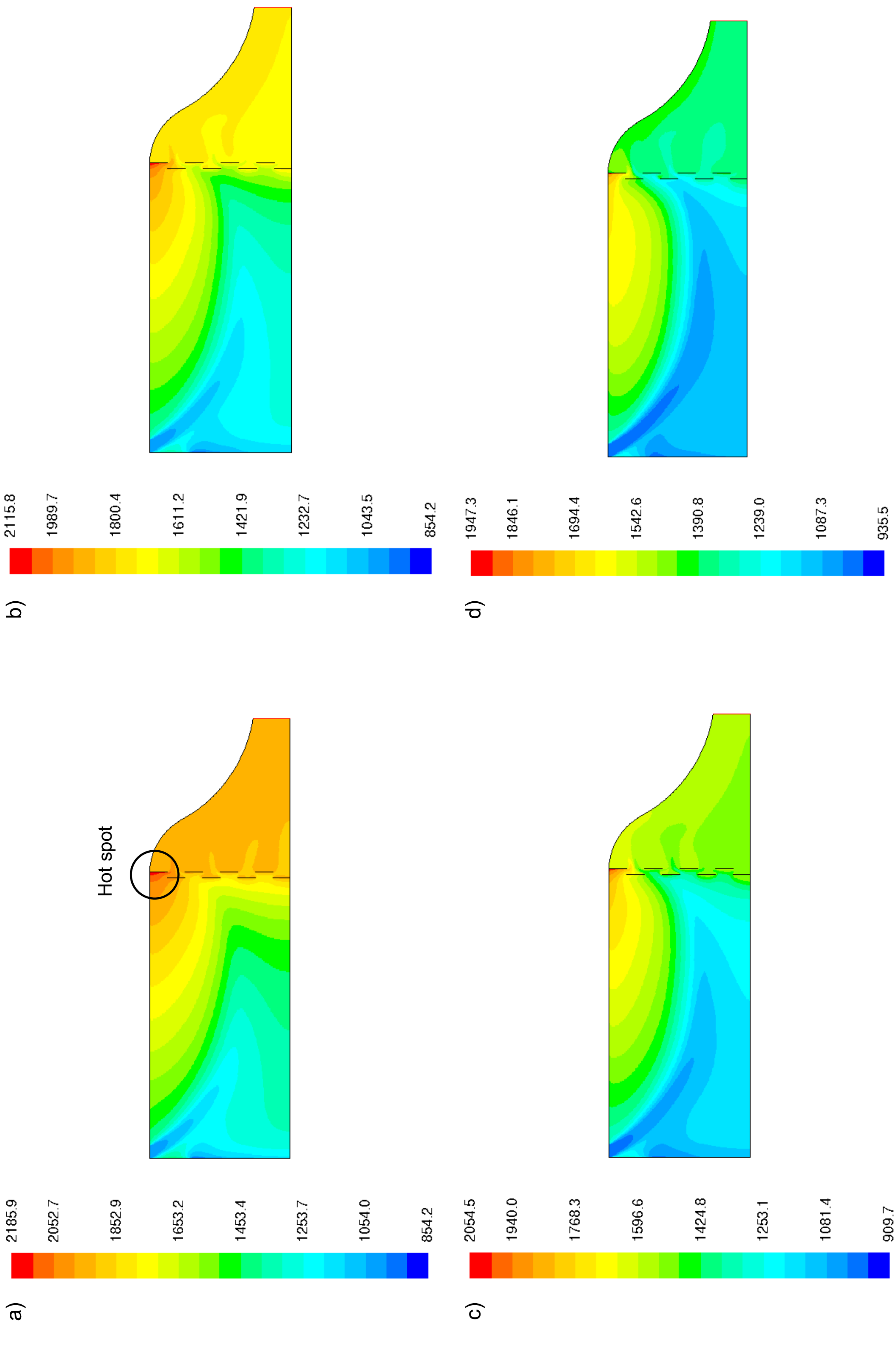

Figure 9: Temperature contours within the receiver for some HTF mass flow rates considered: a) 37.8 kg/s, b) 51.3 kg/s, c) 71.8 kg/s and d) 111.7 kg/s. Temperature values are [K].

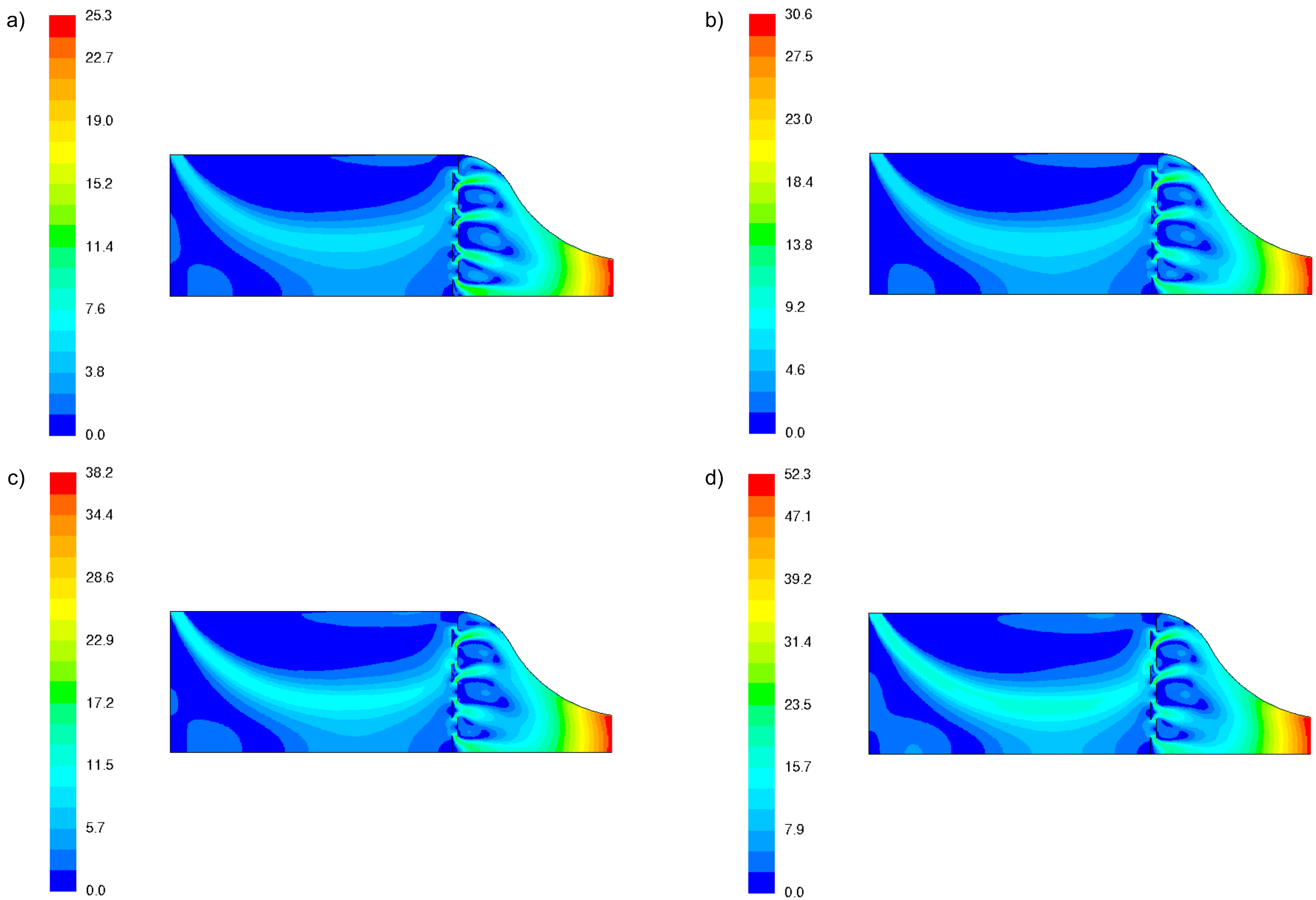

Figure 10: HTF contours of velocity magnitude for some of the mass flow rates considered: a) 37.8 kg/s, b) 51.3 kg/s, c) 71.8 kg/s and d) 111.7 kg/s. Velocity values are [m/s].

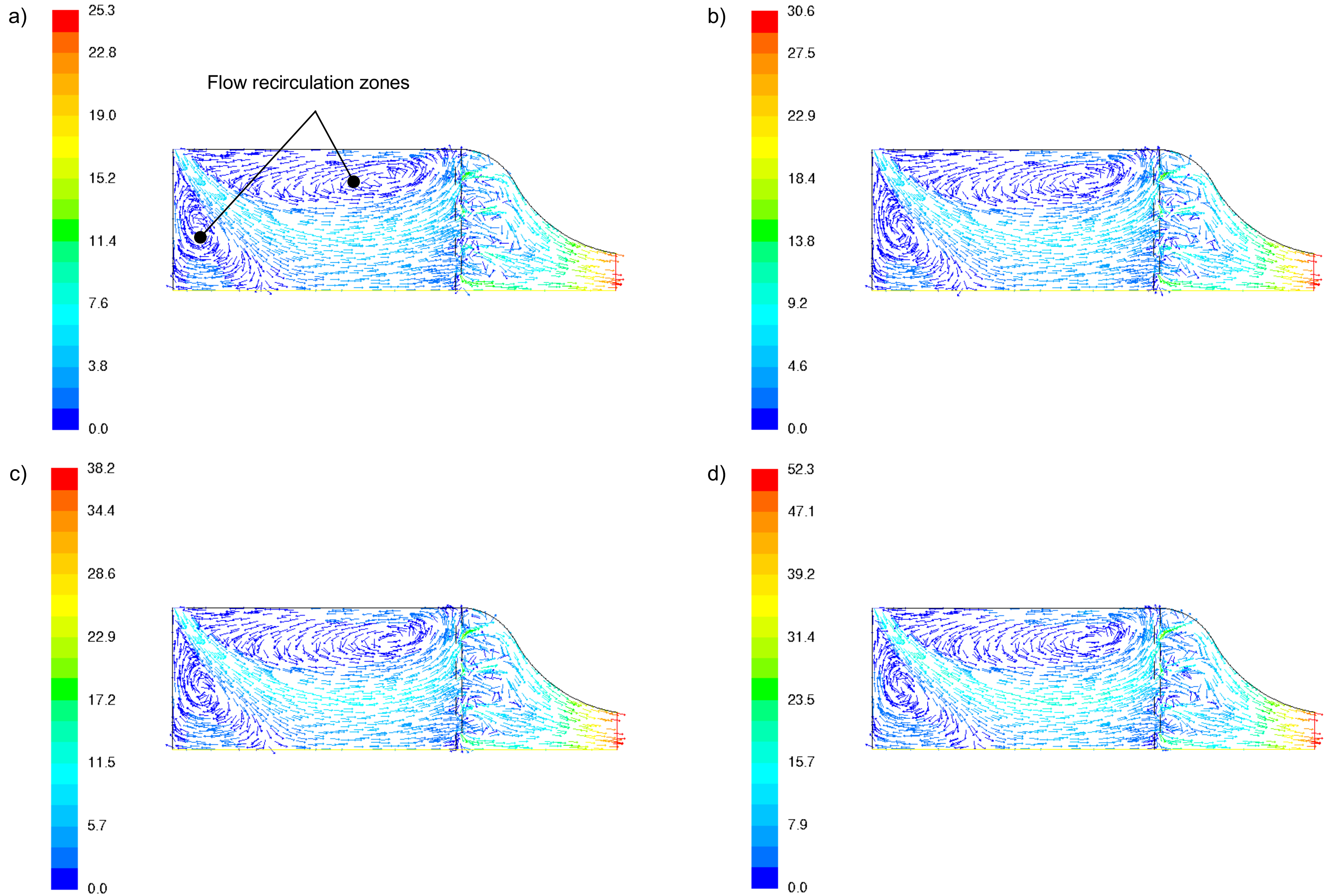

Figure 11: HTF velocity vectors coloured by velocity magnitude for some of the mass flow rates considered: a) 37.8 kg/s, b) 51.3 kg/s, c) 71.8 kg/s and d) 111.7 kg/s. Velocity values are [m/s].

4.2 Pressurized receiver

Pressurized solar receivers are intrinsically more complex than atmospheric pressure receivers especially from the point of view of the pressure-induced mechanical stresses into the quartz-glass aperture window. On the other hand, a relevant advantage of pressurized receivers using gaseous HTFs is the higher density of the working fluid, which enables higher piping system compactness and lower insulation material use. In addition, increasing the operating pressure allows for downscaling the cavity size of the absorbing gas receiver while maintaining a sufficient number of gas molecules for absorption of thermal radiation. For these reasons, in this CFD simulations campaign, the thermo-fluid dynamics behaviour of a pressurized receiver, operating at 10 bars absolute pressure, is accurately evaluated.

The same receiver geometry, described in figure 7, is considered for this analysis with the only exception that the dimensions are downsized with a scaling factor of 22.36. Therefore, the cavity domain of the pressurized receiver is characterized by an internal radius of about 0.36 m and an internal length of 0.72 m leading to a back plate surface area of 0.4 m^2 and a gas volume of 0.293 m^3 (several orders of magnitude lower than that of the atmospheric receiver). Table 3 summarizes the main boundary and operating conditions exploited for the simulations campaign.

Table 3: Summary of the main boundary conditions considered for the simulations campaign.

HTF		
density	ideal gas	[kg/m^3]
viscosity, thermal conductivity, specific heat	f(T) polynomial	[…]
mass flow rate (min. - max.)	0.07 – 0.92	[kg/s]
inlet temperature	1’000	[K]
inlet angle (from aperture)	27	[°]
inlet velocity (min. - max.)	0.48 – 6.3	[m/s]
Radiative heat transfer		
Back plate:		
concentrated solar heat flux / power on cavity side	600 / 240	[kW/m^2] / [kW]
cavity side emissivity	1	[-]
rear domain side emissivity	0	[-]
Lateral wall:		
concentrated solar heat flux / power on cavity side	0 / 0	[kW/m^2] / [kW]
cavity side emissivity	1	[-]
rear domain side emissivity	0	[-]
Operating conditions		
absolute pressure	10	[bar]
ambient temperature	300	[K]

The resulting pressurized receiver thermal efficiency as a function of the HTF outflow temperature is reported, along with those of the reference configuration (atmospheric pressure) and the idealized receiver geometry (validation process) in figure 12. By looking at the results obtained, it is possible to observe that, despite the downsizing factor of the receiver was roughly double with respect to the operating pressure increase, the evolution of the pressurized receiver thermal efficiency has the same trend as the receiver operating at ambient pressure. At low HTF mass flow rates, a more pronounced performance reduction of the pressurized receiver (roughly a 6% reduction at most for the lowest HTF mass flow rate considered) can be detected. Nevertheless, the expected pressurized receiver performance also seems to be very promising.

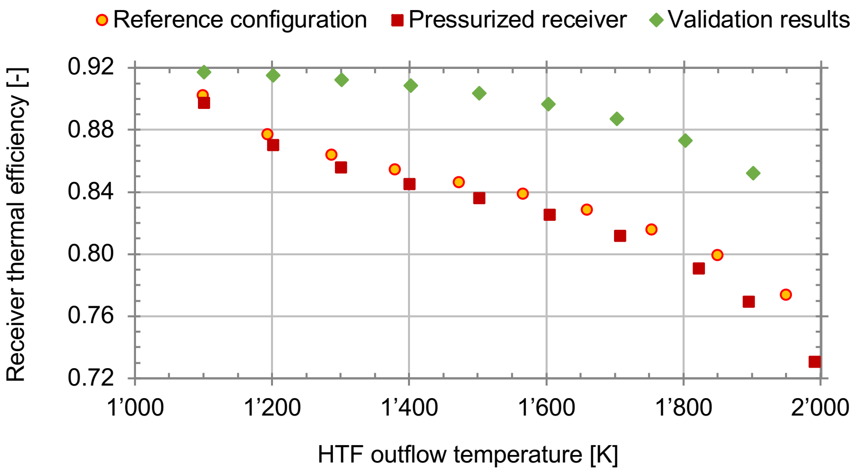

Figure 12: Variation of the receiver thermal efficiency as a function of the HTF outflow temperature for the pressurized receiver.

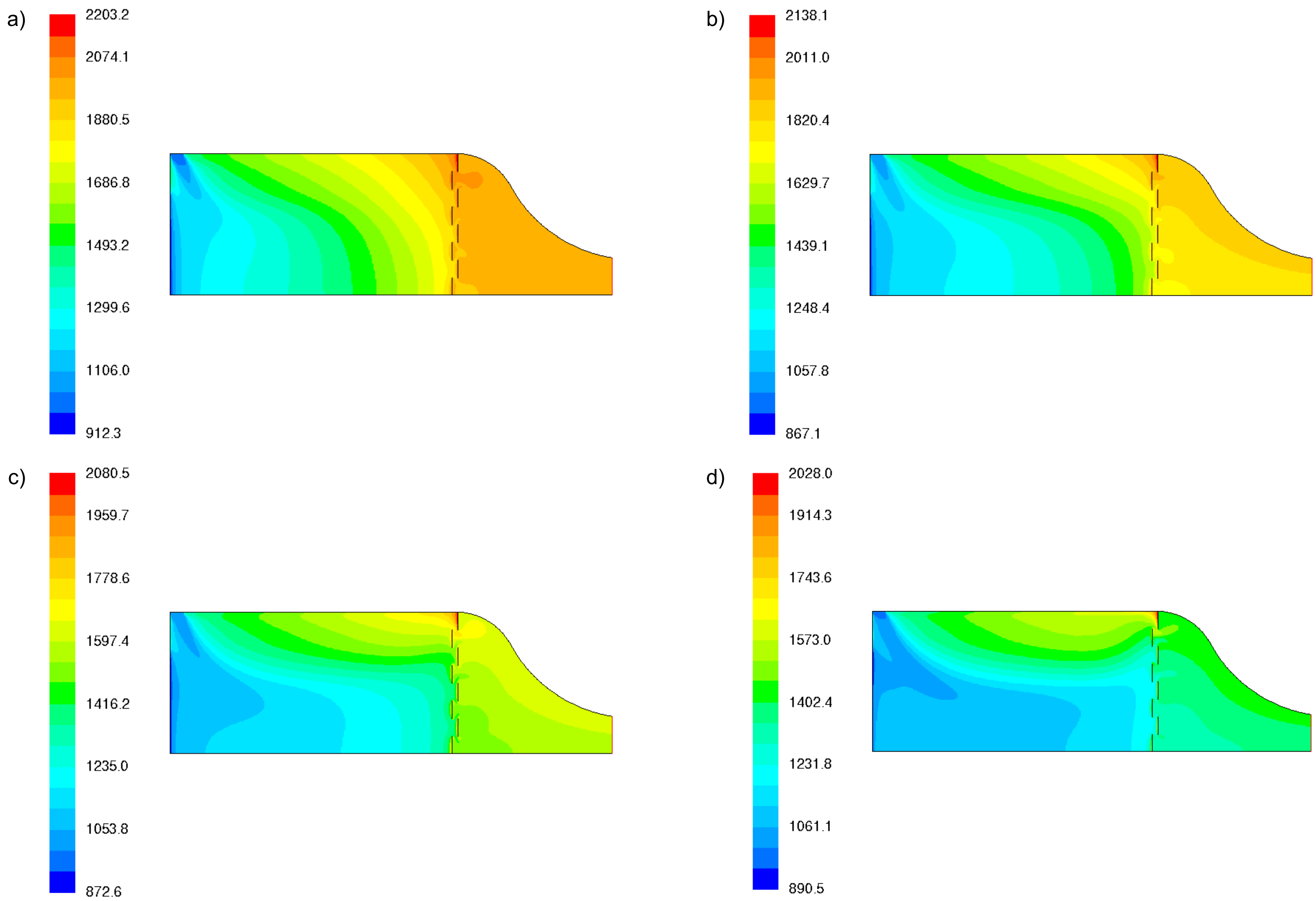

Figure 13: -Temperature contours within the pressurized receiver for some HTF mass flow rates considered: a) 0.07 kg/s, b) 0.09 kg/s, c) 0.13 kg/s and d) 0.21 kg/s. Temperature values are [K].

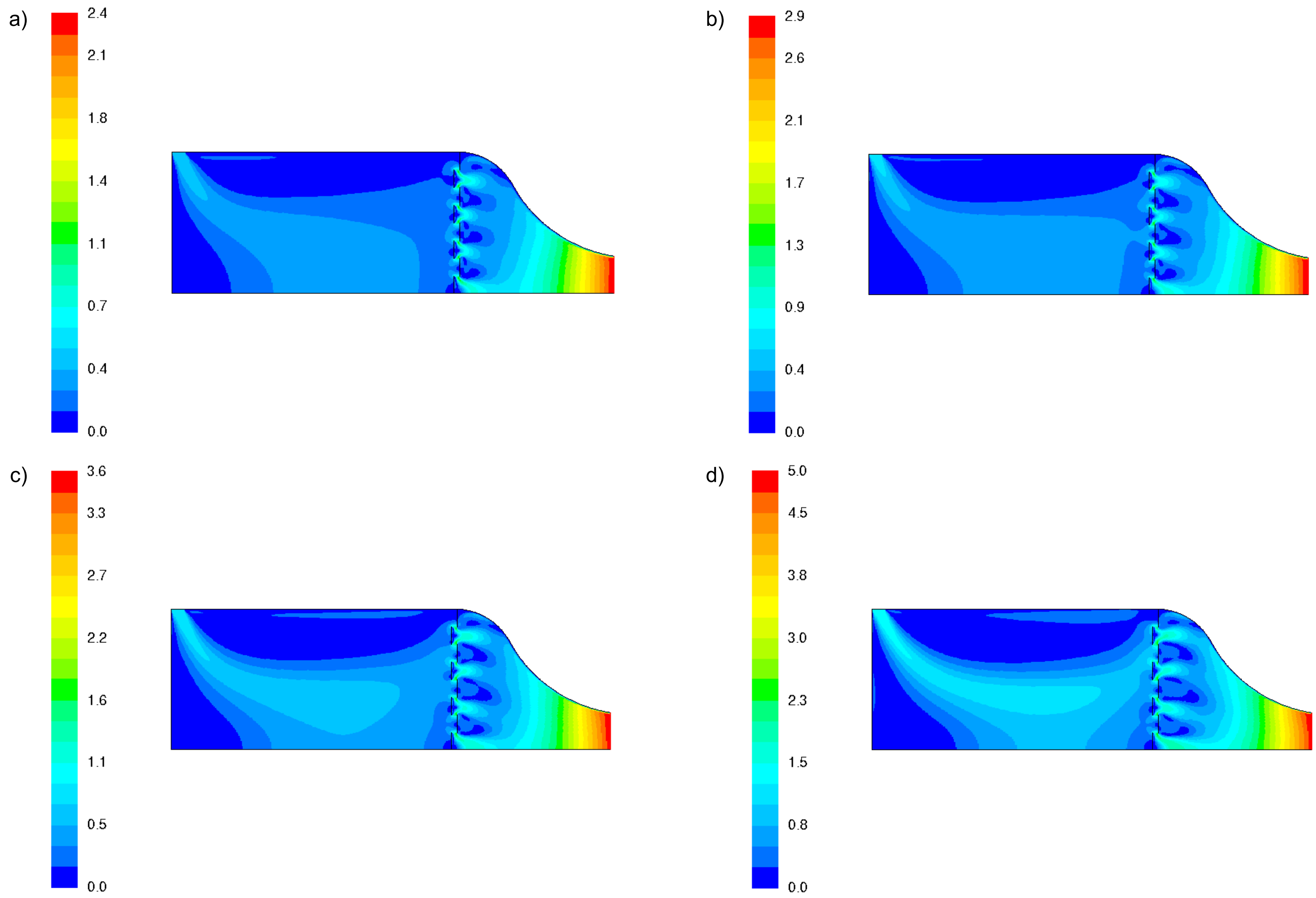

Figure 14: Contours of the velocity magnitude into the pressurized receiver for some of the mass flow rates considered: a) 0.07 kg/s, b) 0.09 kg/s, c) 0.13 kg/s and d) 0.21 kg/s. Velocity values are [m/s].

5 Summary and conclusions

A CFD-based approach was developed with the aim of replicating the thermo-fluid dynamics behavior of the innovative absorbing gas receiver proposed by Synhelion SA. Since this receiver relies on a gaseous HTF to absorb long wavelength thermal radiation, emitted by the internal surfaces of the receiver, the topic of modeling radiative heat transfer in participating media was introduced. The major modeling approaches to solve the RTE, and to account for the spectral variations of the participating media radiation properties, were described. Discrete ordinates method, for solving the RTE, and the WSGG model, for replicating the HTF spectral properties, resulted to be a viable compromise between expected accuracy of the results, computational resources, and computing time.

The CFD model, developed with Fluent code from ANSYS, was validated against benchmark results obtained, by Synhelion, exploiting Monte Carlo ray-tracing and spectral line-by-line models which are the most accurate and realistic methods available. Despite a resulting slight overestimation of the receiver performance (5.4% at most), observed during the validation process, the simplified CFD modeling approach resulted to be an appropriate solution for minimizing the computational resources required by keeping, at the same time, a reasonable accuracy of the results.

Once demonstrated the capability of the CFD model to replicate the physics phenomena governing the absorbing gas receiver behavior, the effect of important working parameters (e.g. operating pressure) on the receiver performance were evaluated. For all the CFD simulations campaign, detailed evaluations and comments on the results were reported in the specific paragraphs; however, as a general consideration, despite the high operating temperature up to 2'000 K, promising receiver performances were observed for all the cases analyzed.

6 References

[1] G. Ambrosetti and P. Good, "A novel approach to high temperature solar receivers with an absorbing gas as heat transfer fluid and reduced radiative losses," *Submitted.*

[2] "ReceiverSIM - Modelling of absorbing gas receiver for solar applications," Annual report, 2017.

[3] M. Modest, Radiative heat transfer - Third edition, Academic Press, 2013.

[4] T. Smith, Z. Shen and J. Friedman, "Evaluation of coefficients for the weighted sum of gray gases model," *J. Heat Transfer,* vol. 104, no. 4, pp. 602-608, 1982.

[5] H. Versteeg and W. Malalasekera, An introduction to computational fluid dynamics: the finite volume method, Harlow, England: Longman Scientific and Technical, 1995.

[6] S. Patankar, Numerical heat transfer and fluid flow, 1980.

National cooperation

None

International cooperation

None

Overall project evaluation

As reported in the Gantt chart, the project covered a total of 9 months during which all the activities proposed have been completed and the various objectives successfully achieved as initially planned.